Crystal Structure and Magnetic Properties of $Ca_2MnAlO_{5.5}$, an $n = 3$ Brownmillerite Phase

Helen M. Palmer, Alan Snedden, Adrian J. Wright, and Colin Greaves*

School of Chemistry, University of Birmingham, Edgbaston, Birmingham, West Midlands B15 2TT, United Kingdom

Received September 22, 2005

The first bulk $n = 3$ brownmillerite structure $Ca_2MnAlO_{5.5}$ has been synthesized by high-pressure oxidation of the $n = 1$ brownmillerite phase, Ca_2MnAlO_5, such that alternate AlO_4 tetrahedral layers are oxidized to AlO_6 octahedra. Rietveld analysis of room-temperature neutron powder diffraction (NPD) data shows a body-centered material (*Imma*, $a = 5.2860(1)$ Å, $b = 29.5334(6)$ Å, $c = 5.4027(1)$ Å). Although magnetic measurements detected an increase in antiferromagnetic ordering at around 40 K, low-temperature NPD measurements implied the presence of no long-range magnetic order.

Introduction

Manganese oxide based materials have been of interest for some time due to their colossal magnetoresistive behavior. This behavior is of great value because of potential applications in magnetic data storage and switching devices. Whereas cubic or pseudo-cubic materials require very high magnetic fields to induce large changes in electrical resistivity, greater sensitivity can be found in systems of lower dimensionality,[1] and this has prompted a great deal of research in various layered structure types containing manganese.

The pioneering work of Jonker and van Santen in the 1950s highlighted the influence of magnetic field on electrical resistivity in three-dimensional ferromagnetic perovskite oxides.[2,3] Further work in this area revealed that enormous changes in electrical resistivity could be achieved close to ambient temperatures by using very high magnetic fields.[4,5] Investigations of low-dimensional materials, such as the $n = 2$ Ruddlesden−Popper phases, have shown similar effects at lower fields.[1,6] Although the observed effects occur at lower temperatures, they clearly indicate the potential of layered manganese oxide systems. One such system is based on the brownmillerite structure, a defect perovskite possessing ordered oxygen vacancies which result in alternating layers of octahedra and tetrahedra; the composition may be represented as $A_2B_2O_5$.[7,8] For relevant magnetic materials, the reduction of dimensionality may be achieved through alternation of magnetic cations, typically Mn, in the octahedral layer and diamagnetic cations in the tetrahedral layer.[9−13]

Previous attempts to obtain bulk, ordered $n = 3$ brownmillerites (where the tetrahedral layer is separated by three octahedral layers) have proven unsuccessful. The reported work to date has focused on the oxidation of the Sr_2MnGaO_5 to the $Sr_2MnGaO_{5.5}$ phase.[9,14−17] The reported results indicate that although the insertion of the oxygen is facile and control of the degree of oxygen incorporation has been achieved, control of the site of oxidation has not been possible, resulting in a disordered oxygen deficient perovskite phase. In this work we will focus on the oxidation of the Ca_2MnAlO_5 structure to a resultant $Ca_2MnAlO_{5.5}$ phase. Neutron powder diffraction (NPD) data reveal an ordered insertion of oxygen, resulting in the first $n = 3$ bulk ordered brownmillerite phase.

* Corresponding author. Telephone: +44 121 4144397. Fax: +44 1214446. E-mail address: c.greaves@bham.ac.uk.

(1) Moritomo, Y.; Asamitsu, A.; Kuwahara, H.; Tokura, Y. *Nature* **1996**, *380*, 141.
(2) Jonker, G. H.; van Santen, J. H. *Physica* **1950**, *16*, 337.
(3) van Santen, J. H.; Jonker, G. H. *Physica* **1950**, *16*, 599.
(4) Raveau, B.; Maignan, A.; Caignaert, V. *J. Solid State Chem.* **1995**, *117*, 424.
(5) Rao, C. N. R.; Cheetham, A. K.; Mahesh, R. *Chem. Mater.* **1996**, *8*, 2421.
(6) Battle, P. D.; Green, M. A.; Laskey, N. S.; Milburn, J. E.; Rosseinsky, M. J.; Sullivan, S.; Vente, J. P. *Chem. Commun.* **1996**, *6*, 767.
(7) Bertaut, E. F.; Blum, P.; Saignieres, A. *Acta Crystallogr.* **1959**, *12*, 149.
(8) Coville, A. A.; Geller, S. *Acta Crystallogr., Sect. B* **1971**, *27*, 2311.
(9) Abakumov, A. M.; Rozova, M. G.; Pavlyuk, B. P.; Lobanov, M. V.; Antipov, E. V.; Lebedev, O. I.; van Tendeloo, G.; Ignatchik, O. L.; Ovtchenkov, E. A.; Koksharov, Y. A.; Vasil'ev, A. N. *J. Solid State Chem.* **2001**, *160*, 353.
(10) Abakumov, A. M.; Rozova, M. G.; Pavlyuk, B. P.; Lobanov, M. V.; Antipov, E. V.; Lebedev, O. I.; van Tendeloo, G.; Sheptyakov, D. V.; Balagurov, A. M.; Bouree, F. *J. Solid State Chem.* **2001**, *158*, 100.
(11) Wright, A. J.; Palmer, H. M.; Anderson, P. A.; Greaves, C. *J. Mater. Chem.* **2001**, *11*, 1324.
(12) Wright, A. J.; Palmer, H. M.; Anderson, P. A.; Greaves, C. *J. Mater. Chem.* **2002**, *12*, 978.
(13) Battle, P. D.; Bell, A. M. T.; Blundell, S. J.; Coldea, A. I.; Fallon, D. J.; Pratt, F. L.; Rosseinsky, M. J.; Steer, C. A. *J. Solid State Chem.* **2002**, *167*, 188.
(14) Pomjakushin, V. Y.; Balagurov, A. M.; Elzhov, T. V.; Sheptyakov, D. V.; Fischer, P.; Khomskii, D. I.; Yushankhai, V. Y.; Abakumov, A. M.; Rozova, M. G.; Antipov, E. V.; Lobanov, M. V.; Billinge, S. J. L. *Phys. Rev. B* **2002**, *66*, 184412.
(15) Antipov, E. V.; Abakumov, A. M.; Alekseeva, A. M.; Rozova, M. G.; Hadermann, J.; Lebedev, O. I.; van Tendeloo, G. *Phys. Status Solidi* **2004**, *201*, 1403.
(16) Pomajakushin, V.; Sheptyakov, D.; Fischer, P.; Balagurov, A.; Abakumov, A.; Alekseeeva, M.; Rozova, M.; Antipov, E.; Khomskii, D.; Yushankhai, V. *J. Magn. Magn. Mater.* **2004**, *272−276*, 820.
(17) Caspi, E. N.; Avdeev, M.; Short, S.; Jorgensen, J. D.; Dabrowski, B.; Chmaissem, O.; Mais, J.; Kolesnik, S. *J. Solid State Chem.* **2004**, *177*, 1456.

10.1021/cm052134n CCC: $33.50
Published on Web 02/04/2006

Table 1. Refined Structural Parameters for $Ca_2MnAlO_{5.5}$ Obtained from Rietveld Analysis of Powder Neutron Diffraction Data (295 K)[a]

atom	site	multiplicity	x	y	z	$U_{iso} \times 100$, Å^2	occupancy
Ca1	2/M(100)	8	0	0.058 26(5)	0.5051(3)	1.03(3)	1
Ca2	M(100)	8	0	0.320 06(6)	0.5268(3)	0.77(3)	1
Mn	M(100)	8	0	0.125 83(6)	0.0051(4)	0.61(3)	1
Al1	2/M(100)	8	0	0	0	0.86(5)	1
Al2	M(010)	4	0.0515(6)	0.25	0.0740(7)	0.50(7)	0.5
O1	2(010)	8	0.25	−0.006 06(5)	0.25	0.99(2)	1
O2	2(010)	8	0.25	0.137 22(4)	0.25	0.62(2)	1
O3	2(010)	8	0.25	0.621 35(5)	0.25	0.80(2)	1
O4	M(100)	8	0	0.065 59(5)	0.0625(2)	0.96(2)	1
O5	M(100)	8	0	0.302 90(5)	−0.0595(3)	0.90(3)	1
O6	M(010)	8	0.1146(4)	0.25	0.3630(4)	0.50(3)	0.5

[a] $R_{wp} = 2.12\%$, $R_p = 3.65\%$, $\chi^2 = 4.049$. *Imma*: $a = 5.2860(1)$ Å, $b = 29.5334(6)$ Å, $c = 5.4027(1)$ Å.

Experimental Section

A sample of $Ca_2MnAlO_{5.5}$ was prepared from Ca_2MnAlO_5. Ca_2MnAlO_5 was prepared, as previously reported,[12] by firing a stoichiometric mixture of $CaCO_3$, Mn_2O_3, and Al_2O_3 for 48 h at 1250 °C under flowing nitrogen with one intermediate regrind. Ca_2MnAlO_5 was subsequently heated at 600 °C under a 300 bar oxygen pressure for 12 h to produce $Ca_2MnAlO_{5.5}$. Phase purity was established using X-ray powder diffraction (XRPD, Siemens D5000, PSD, Ge monochromator, Cu Kα_1 radiation). Room-temperature NPD data were collected on POLARIS at ISIS. The obtained data were analyzed using the GSAS[18] suite of programs. Oxygen content determination was performed by thermogravametric analysis (TGA; Rheometric STA 1500 thermal analyzer) by reduction in flowing 10% H_2/90% N_2 to the Ca_2MnAlO_5 phase. Magnetic measurements were carried out on a Quantum Design Physical Property Measurement System (PPMS) at 10 000 Oe.

Results and Discussion

From the laboratory XRPD data it was clear that the structure of the sample had significantly changed after oxidation; although the sample could be indexed on a tetragonal unit cell, $2a_p \times 2a_p \times a_p$ ($a_p = a$ for cubic perovskite), it did not appear to be a simple perovskite. The extent of oxygen content of the sample was determined by TGA and established as 5.5. It was deemed reasonable at this stage that the structural change could be due to oxygen ordering, although this could not be established accurately using X-ray diffraction. NPD data were, therefore, collected.

The Rietveld refinement of the powder data was performed using the high-resolution backscattering bank only; the details and results of this refinement are given in Table 1, and a plot of the fit to the data is shown in Figure 1. Selected bond distances and angles are given in Table 2. The data confirm that the structure is indeed a brownmillerite type phase with ordered oxygen vacancies. Here we describe the structure using *Imma* symmetry, which is the standard space group setting for the *Icmm* space group, previously used to describe "chain-disordered" structures such as Sr_2MnGaO_5.[12] Refinements carried out in the "chain-ordered" *I*2*mb* space group (equivalent to *Ima*2, but chosen to retain the unit cell axes) were found to be less satisfactory ($\chi^2 = 4.049$, 4.931; $R_{wp} = 2.12\%$, 2.34%; and $R_p = 3.65\%$, 4.13% for *Imma* and *I*2*mb*, respectively). From the space group selection it can be understood that the chains remain ordered along the [001] direction but are disordered with respect to the two possible chain orientations (for more detail see Greaves et al.).[12] This disorder is reflected in the 50% occupancy of the Al2 and O6 sites within the tetrahedral layers (Table 1).

Table 2. Selected Bond Lengths (Å) and Bond Angles (deg) for $Ca_2MnAlO_{5.5}$

Mn−O2	1.900(2) [×2]	Ca1−O1	2.694(2) [×2], 2.424(2) [×2]
Mn−O3	1.914(2) [×2]	Ca1−O2	3.014(2) [×2]
Mn−O4	1.806(3)	Ca1−O3	2.640(2) [×2]
Mn−O5	2.134(2)	Ca1−O4	2.6769(3) [×2], 2.401(2), 3.020(2)
Al1−O1	1.8981(1) [x4]	Ca2−O2	2.361(2) [×2]
Al1−O4	1.966(2) [×2]	Ca2−O3	2.489(2) [×2]
Al2−O5	1.742(2) [×2]	Ca2−O5	2.697(4) [×2]
Al2−O6	1.791(4), 1.798(4)	Ca2−O6	2.331(2) [×2]
O2−Mn−O2	88.1(1)	O1−Al1−O1	88.249(8), 180.0
O2−Mn−O3	173.68(1), 91.92(1)		91.751(8)
O2−Mn−O4	93.12(9)	O1−Al1−O4	88.32(5), 91.68(5)
O2−Mn−O5	86.52(8)	O4−Al1−O4	179.972(1)
O3−Mn−O3	87.3(15)	O5−Al2−O5	127.5(2)
O3−Mn−O4	93.12(9)	O5−Al2−O6	106.5(1), 103.4(1)
O3−Mn−O5	87.17(9)		115.9(1)
O4−Mn−O5	179.501(1)	O6−Al2−O6	41.4(2), 67.0(2), 108.4(2)

The ordered insertion of oxygen into the structure directly contrasts to the behavior of the $Sr_2MnGaO_{5.5}$ phase, where no order is observed.[9,14−17] The reasons for the divergence of behavior in these two analogous compounds can most likely be attributed to the differences between the ionic radii of the cations involved (Ca^{2+}, 1.34 Å; Sr^{2+}, 1.44 Å; Al^{3+}, 0.39 Å; Ga^{3+}, 0.47 Å). The smaller size of the cations in the calcium containing phase creates a more compact lattice with a larger energy barrier to oxidation, explaining the need for

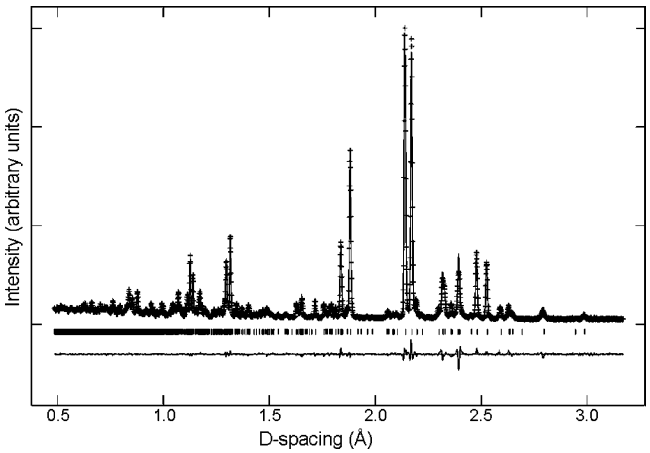

Figure 1. NPD profile (continuous lines, calculated and difference; crosses, observed data) for $Ca_2MnAlO_{5.5}$ at 295 K and backscattering bank data. The tick marks indicate the reflection positions.

(18) Larson, A. C.; von Dreele, R. B. *General Structure Analysis System*; Los Alamos National Laboratory: Los Alamos, NM, 1994.

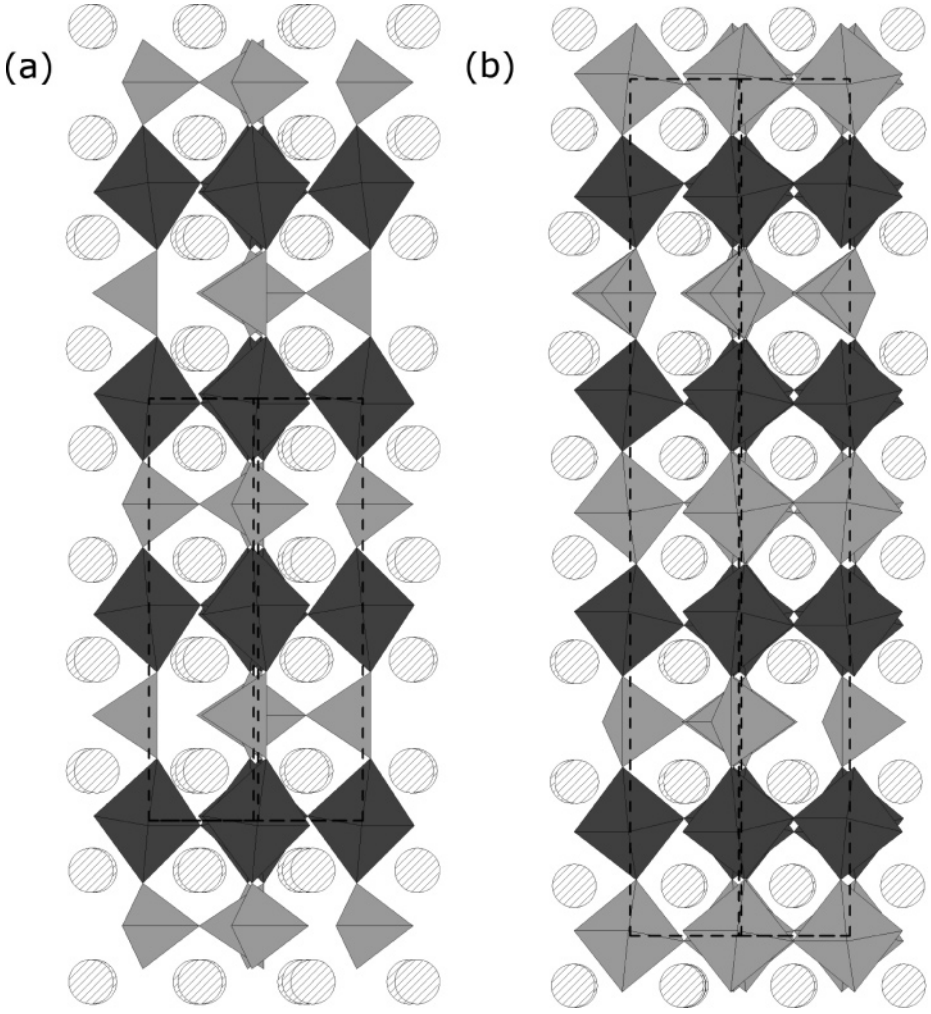

Figure 2. Structures of (a) Ca_2MnAlO_5 and (b) $Ca_2MnAlO_{5.5}$ showing Ca (large spheres) with MnO_6 octahedra (dark gray) and AlO_6 and AlO_4 octahedra and tetrahedra (light gray).

much harsher synthesis conditions. The oxygen ordering is also likely to be directly attributable to the size of the cations: the larger size of Sr^{2+} compared with Ca^{2+} might reduce the energy barrier for oxygen migration and also reduce the enthalpy associated with vacancy ordering. Similar behavior is observed in the synthesis of the $Ca_2Fe_2O_5$ and $Sr_2Fe_2O_5$ brownmillerite phases. The Ca containing phase can be made in air and will not readily accept excess oxygen, whereas the Sr containing phase has to be heated in nitrogen to obtain the $Sr_2Fe_2O_5$ phase.[19] This difference of behavior might provide a means of fine-tuning the oxygen insertion capabilities of mixed Ca/Sr brownmillerite phases.

A comparison between the non-oxidized and oxidized samples reveals several interesting and subtle structural features of the oxidized system. It is clear from the space groups and prior discussion that the oxidized sample has disordered chains, whereas prior work[12] revealed that Ca_2MnAlO_5 has ordering of the chains. This loss of chain order with respect to the two rotations of the chains is not the only change occurring in the AlO_4 layers upon oxidation. As a result of the body-centered nature of the *I*2*mb* space group, the AlO_4 tetrahedral layers are staggered by ($x + 1/2$, $y + 1/2$, $z + 1/2$); this is most apparent when viewed along [001] due to the lack of connectivity along *c*. When considering the oxidized sample, the body centering provides similar staggering of the AlO_4 tetrahedral layers. As the alternate tetrahedral layers in the oxidized sample are equivalent to, for example, the first and third layers of the Ca_2MnAlO_5 phase, this means that a restructuring of the oxygen vacancies in the oxidized sample has taken place, as illustrated in Figure 2. This restructuring may point to a systematic behavior in brownmillerite phases: those with an odd number of layers having a staggered layer order and those with even layers having an eclipsed layer order. This is most probably due to the tilting of the octahedral layers. It can be suggested that the oxygen atoms in the tetrahedral layer are positioned to place them far away from the octahedral atoms in the *ac* plane to minimize the energy of the system; a schematic of this is shown in Figure 3. It is acknowledged that until now only the $n = 1$ and $n = 2$ phases have been characterized and that as of yet no $n \geq 4$ phases are known.

Upon oxidizing the sample it would be expected that the Mn−O bonds would decrease in length as the Mn cation is oxidized from 3+ to 4+. It would also be expected that the change from tetrahedral to octahedral geometry would cause an expansion in the relevant Al−O bonds. Indeed both of these structural changes are observed. An examination of

(19) Berastegui, P.; Eriksson, S.-G.; Hull, S. *Mater. Res. Bull.* **1999**, *34*, 303.

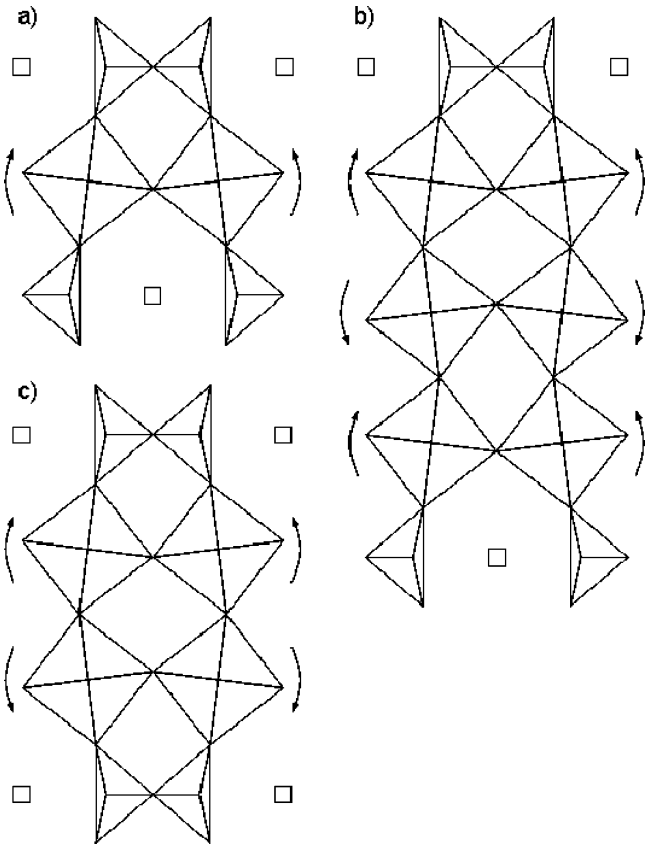

Figure 3. Schematic representation of octahedral tilting and ordering of oxygen vacancies in $n = 1$, 2, and 3 brownmillerites (a, b, and c respectively). Arrows indicate direction of tilting; boxes indicate oxygen vacancies.

the bond valence sum (BVS)[20] for the oxidized sample shows that both the tetrahedral and the octahedral sites correspond to Al^{3+} (BVS: 2.89, 2.87, respectively). For the manganese site the BVS calculation gives a value of 3.81 a substantial increase on the value of 3.29 for Ca_2MnAlO_5. The only site to indicate strain is the Ca2 site which gave a BVS value of 2.26; this site is bonded to oxygen atoms in the disordered Al−O layer, and this may result in an inaccurate value. It seems from these values that there is relatively little strain within the structure.

From the plot of magnetic susceptibility versus temperature (Figure 4) very little difference is observed between the field cooled and zero field cooled lines. The extrapolated intercept of the inverse susceptibility plot (Figure 5) suggests predominantly antiferromagnetic exchange at high temperatures; the marked change of slope at ∼40 K is consistent with a ferromagnetic component, e.g. a canted antiferromagnetic

(20) Brown, I. D.; Altermatt, D. *Acta Crystallogr., Sect. B* **1985**, *41*, 244.

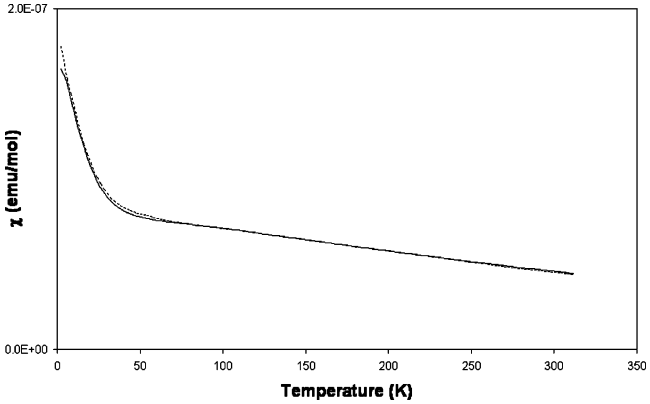

Figure 4. Plot of susceptibility versus temperature for $Ca_2MnAlO_{5.5}$.

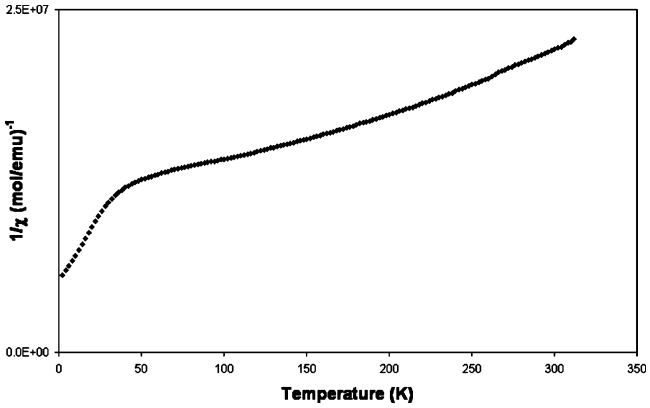

Figure 5. Plot of inverse susceptibility versus temperature for $Ca_2MnAlO_{5.5}$.

structure. However, NPD data collected at 2 K revealed no evidence of long-range magnetic order, and it is therefore probable that magnetic interactions provide only two-dimensional intralayer antiferromagnetic order within the manganese layers.

Conclusions

In conclusion we have successfully synthesized the first $n = 3$ brownmillerite phase in bulk form: $Ca_2MnAlO_{5.5}$ has alternating tetrahedral and octahedral Al−O layers, with each layer being separated by an octahedral Mn−O layer. The unexpected staggered conformation of the tetrahedral layers is attributed to the tilting found in the octahedral layers and consequent energy minimization. The structure while having some increase in local antiferromagnetic order was not found to possess any long-range magnetic ordering.

Acknowledgment. We thank the EPSRC for funding (A.S. and H.M.P.) and Ron Smith for help with NPD data collection.

CM052134N